Journal of Hazardous Materials 489 (2025) 137653

Contents lists available at ScienceDirect

Journal of Hazardous Materials

journal homepage: www.elsevier.com/locate/jhazmat

Ecotoxicity of the non-dioxin-like PCB-153 in the model marine diatom *Phaeodactylum tricornutum*

Bernardo Duarte [a,b,*], João Cardoso [a,c], Eduardo Feijão [a,d], João Albuquerque Carreiras [a,d], Ricardo Cruz de Carvalho [a,e], Ana Rita Matos [b,d], Vanessa F. Fonseca [a,f], Paula Santos [c], Carla Palma [c]

[a] MARE – Marine and Environmental Sciences Centre/ ARNET – Aquatic Research Network, Faculdade de Ciências, Universidade de Lisboa, Campo Grande, Lisboa 1749-016, Portugal
[b] Departamento de Biologia Vegetal, Faculdade de Ciências da Universidade de Lisboa, Campo Grande, Lisboa 1749-016, Portugal
[c] Instituto Hidrográfico, Rua das Trinas 49, Lisboa 1249-093, Portugal
[d] BioISI – Instituto de Biossistemas e Ciências Integrativas, Departamento de Biologia Vegetal, Faculdade de Ciências da Universidade de Lisboa, Campo Grande, Portugal
[e] cE3c—Center for Ecology, Evolution and Environmental Changes & CHANGE—Global Change and Sustainability Institute, Faculdade de Ciências da Universidade de Lisboa, Campo Grande, Lisboa 1749-016, Portugal
[f] Departamento de Biologia Animal, Faculdade de Ciências da Universidade de Lisboa, Campo Grande, Lisboa 1749-016, Portugal

HIGHLIGHTS

- PCB-153 exposure impairs Photosystem II and diatom growth at environmental levels.
- PCB-153 accumulation leads to oxidative stress, despite antioxidant responses.
- Photosystem II parameters and photochemical index strongly correlate with PCB-153 dose.
- Exposure biomarkers included pheophytin a, fucoxanthin, catalase activity, and growth inhibition.

GRAPHICAL ABSTRACT

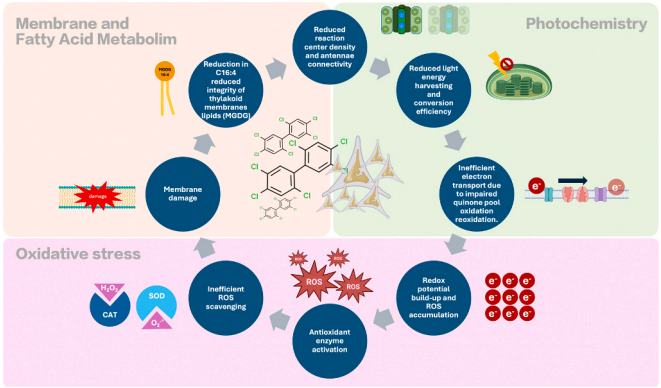

ARTICLE INFO

Keywords:
Polychlorinated biphenyls
Toxicophenomics
Oxidative stress
Marine diatoms

ABSTRACT

Despite the ban on polychlorinated biphenyls (PCBs) in developed countries since the 1930s, their persistence and use endured in developing countries, with reported toxic effects on various organisms. PCB congener 153 (PCB-153, 2, 2′, 4, 4′, 5, 5′–hexachlorobiphenyl) is notably prevalent in marine biota. However, its mode of action and impact on primary marine diatoms are not well documented. *Phaeodactylum tricornutum* cultures exposed to environmentally relevant PCB-153 levels (0, 1, 3, and 6 µg/L) showed proportional accumulation, impairing photochemical processes by directly affecting the structure and function of Photosystem II and hindering light

* Correspondence to: MARE – Marine and Environmental Sciences Centre, Faculdade de Ciências, Universidade de Lisboa, Campo Grande, Lisboa 1749-016, Portugal.
E-mail address: baduarte@fc.ul.pt (B. Duarte).

https://doi.org/10.1016/j.jhazmat.2025.137653
Received 1 October 2024; Received in revised form 11 February 2025; Accepted 16 February 2025
Available online 17 February 2025

harvesting and electron conversion. This impairment significantly inhibited growth (calculated IC_{25} = 3.53; predicted IC_{50} = 7.09 μg/L) within environmental concentrations, which is linked to oxidative stress despite antioxidant responses and increased fucoxanthin production. The increased pheophytin *a* levels along the PCB-153 gradient further supported this finding. Key biomarkers identified with a direct correlation with the exposed and internalized PCB doses included pheophytin *a*, fucoxanthin, catalase activity, non-photochemical reaction index (SFI [NPQ]), and growth inhibition. PSII functioning parameters (ABS/CS, ET/CS, TR/CS, S_M, and M_o), photochemical reaction index (SFI), and specific growth rate showed strong inverse correlations with the PCB-153 dose. This study provides new insights into PCB-153 ecotoxicity in marine phytoplankton and highlights effective biomarkers for future ecotoxicological assessments of marine diatoms.

1. Introduction

Polychlorinated biphenyls (PCBs) constitute a class of ubiquitous anthropogenic contaminants classified as persistent organic pollutants (POPs). These compounds comprise approximately 209 distinct congeners, each exhibiting specific physicochemical and toxicological properties [1]. Since the 1930s, these compounds have been used in electrical capacitors and transformers, as lubricants, cooling fluids, and hydraulic fluids, as well as in adhesives and plasticizers [2], with approximately 2 million tons of PCBs produced since 1929 [3]. Due to their adverse health and environmental effects, these compounds have been progressively prohibited in numerous countries since 1972, although less stringent regulations persist in developing economies. [3]. It is estimated that approximately 750,000 tons of PCBs are present in the biosphere [4], posing serious reproductive, neurological, and endocrinological risks [5]. Owing to their high resistance to degradation, PCBs are highly persistent in the environment, and because of their lipophilicity, they readily bioaccumulate throughout the trophic web [6].

The PCB congener 153 (PCB-153, 2, 2′, 4, 4′, 5, 5′–hexachlorobiphenyl) is recognized as the most abundant PCB detected in marine biota [1]. PCB-153 exhibits multiple industrial and commercial applications, attributable to its chemical stability and thermal resistance. Consequently, it has been widely produced and used in multiple industrial processes [7] and has been frequently detected. In Galicia, Spain, sediment analysis has revealed higher concentrations of chlorinated PCBs, including PCB-153, particularly in finer sediment fractions [8]. PCB concentrations in the Mediterranean Sea were observed to be highest in the western and central regions, with certain fish and mussel specimens exceeding the Food and Drug Administration (FDA) limit of 2 mg/kg [9]. In another study, PCB-153 levels varied from 7.4 ng/g to 47.5 ng/g in plastic resin pellets from beaches along the Accra-Tema coastline, in Ghana [10]. In aquatic environments, the concentration of this compound fluctuates from a few nanograms per litre [10] to the microgram per litre level in estuarine waters [11]. PCB-153 has been detected in human tissues as the predominant ortho-substituted congener, constituting approximately 30 % of the total PCBs in all analyzed samples [12]. In contrast to several other polychlorinated biphenyl (PCB) congeners, PCB-153 does not exhibit dioxin-like behavior due to its inability to bind to the aryl hydrocarbon receptor [3]. In both animal and human subjects, PCB-153 has been demonstrated to interact with the pregnane X receptor (PXR) and constitutive androstane receptor (CAR), thereby influencing the expression of associated genes, which may potentially result in metabolic dysfunction and pathological conditions [13,14].

The toxicity of this compound has also been examined in algal model organisms, particularly in green algae species such as *Pseudokirchneriella subcapitata* [15] and *Selenastrum capricornutum* [16], emphasizing its adverse effects on these species, especially in relation to growth rates. Nevertheless, data regarding its impact on marine diatoms, the predominant phytoplankton group, remains limited. Diatoms are the cornerstones of marine food webs [17] and are responsible for approximately 20 % of global primary production [18]. They serve as major marine carbon sinks and key oxygen production sources, which are essential for supporting marine heterotrophs [19]. Consequently, any alteration at the photochemical or biochemical level resulting from exposure to contaminants has the potential to provide effective and ecologically relevant biomarkers with implications at the systemic level. In this context, *Phaeodactylum tricornutum* has been adopted as an ecotoxicological model to assess the toxicity of several organic and inorganic contaminants [20] using various analytical techniques such as optical phenotyping techniques [21–23], classical oxidative stress biomarkers [24–26], fatty acid profiling [27,28], and metabolomics [29]. The application of such a diverse array of techniques not only enables the identification of potential biomarkers of exposure to specific compounds but also facilitates the elucidation of the mechanisms of action underlying the effects of the tested substances. The cosmopolitan diatom species growth-rate inhibition test has been routinely employed to assess water quality in marine and brackish environments. [30,31]. The vast knowledge acquired for this species in terms of its biology, ecology and ecotoxicology makes *P. tricornutum* a suitable species for this type of bioassays [32–34]. Furthermore, this species is widely considered a representative model for phytoplankton responses to stressors. Its diminutive size renders it particularly suitable for investigating the effects of chemical stressors on phytoplankton species, as smaller phytoplankton organisms are known to be more substantially affected [30,35]. Recent studies have elucidated the sensitivity of photochemical, oxidative stress, and fatty acid biomarkers of this species to a diverse range of legacy and emerging contaminants [21,22,24,28]. Given the existing research on the ecotoxicity of these compounds, primarily in green algae, their persistence in marine environments, the prevalence of diatoms in marine and transitional ecosystems, and the paucity of information regarding the metabolic effects of PCB-153 on phytoplankton, this represents a significant knowledge gap that warrants further investigation.

Therefore, the present study aimed to assess the effects of realistic PCB-153 concentrations on the accumulation and physiological traits of the diatom species *P. tricornutum*. The objective of this investigation was to elucidate the mechanism of action of this compound in this model organism and to characterize its toxicological effects on this key phytoplankton group. This was accomplished by evaluating *P. tricornutum* growth, energy and fatty acid metabolism, and oxidative stress, along with a biomarker discovery approach to identify potential physiological traits for future ecotoxicological assessments of marine diatoms.

2. Materials and methods

2.1. Exposure trials

In the present work, an axenic monoclonal cell culture of *P. tricornutum* Bohlin (Bacillariophyceae) (strain IO 108–01, Instituto Português do Mar e da Atmosfera (IPMA)) was maintained under asexual reproduction conditions in f/2 medium [36]. The axenic state of the culture was confirmed through periodic visual inspection under a microscope. Exposure trials were conducted as previously described [37]. Briefly, cultures were placed in a phytoclimatic chamber (temperature = 18 °C, 14/10 h day/night photoperiod, maximum PAR = 80 μmol photons m^{-2} s^{-1} (RGB 1:1:1), programmed in a sinusoidal function

to mimic sunrise and sunset, and maximum light intensity at noon). Exposure was carried out according to the Organization for Economic Cooperation and Development (OECD) guidelines for algal assays [38] with minor modifications. The initial cell density was set to 2.7×10^5 cells mL^{-1}, a suitable value for microalgae cells with dimensions analogous to those of *P. tricornutum*. Carbon was supplied by aeration in the ambient air. A 10 mg mL^{-1} PCB-153 (2,2′,4,4′,5,5′-Hexachlorobiphenyl, Sigma-Aldrich, Germany) was used as the stock solution. Following a 48-hour acclimation period, the cultures were supplemented with appropriate volumes of PCB-153 stock solution to achieve the target final concentrations (0, 1, 3, and 6 µg/L). According to the literature [39], this compound is highly persistent and has a lower degradability in aqueous media, thus considering a closed exposure setup. Due to the sample preparation requirements of the culture volumes for the various biochemical assays, PCB-153 concentrations were analyzed exclusively in the diatom cells. While the majority of extant literature focuses on PCB concentrations in sediments, the target dissolved concentrations were selected to encompass a range that reflected realistic environmental concentrations reported in the available literature [11,40]. Although PCBs typically appear at lower concentrations, results from the Seine Estuary report PCB concentrations of 1300 ng/L [11]. This was established as the environmental concentration, and progressive increases simulating elevated contamination scenarios (3 and 6 µg/L) were implemented to evaluate the effects of potentially increasing concentrations within the same order of magnitude as the maximum reported value obtained from the literature. Owing to the fast growth rate of this diatom, the exposure time was reduced to 48 h to avoid artifacts resulting from cell aging observed at 72 h when the cultures entered the stationary phase [37]. Aseptic conditions were maintained by conducting all manipulations within a laminar flow hood chamber. Phaeodactylum tricornutum cell density was quantified utilizing a Neubauer-improved counting chamber under an Olympus BX50 inverted microscope (Tokyo, Japan) (magnification 400 ×).The mean specific growth rate (SGR) per day, doubling time (d, in days), and number of divisions per day (M) were calculated as follows (Eq. 1) [41]:

$$d = \ln\frac{2}{SGR} \text{ and} M = \frac{1}{d} \quad (1)$$

At the end of the 48 h of the exposure period, cells were analyzed photochemically as described below (Section 2.2), centrifuged (4000 × *g* for 15 min at 4 °C), harvested for biochemical analysis, flash-frozen in liquid nitrogen, and stored at −80 °C. All experimental conditions comprised three biological replicates for each analysis, resulting in a total of 12 independent experimental units.

2.2. PCB-153 diatom uptake

PCB 153 was extracted from diatom cells using the QuEChERS methodology [42]. First, a pellet corresponding to 30 mL of culture and known cell density was transferred to a 50 mL tube, and 15 mL of 1 % acetic acid in acetonitrile was added. Subsequently, 4 g of anhydrous magnesium sulfate, 1 g of sodium chloride, 1 g of monosodium citrate, and 0.5 g of sodium citrate dibasic sesquihydrate were added, and the tubes were shaken in a vortex for 1 min and centrifuged at 1500 rpm for 1 min. Subsequently, 5 mL of the supernatant was transferred to another 50 mL tube, and a clean-up salt mixture was added. 150 mg $MgSO_4$ was used to absorb the remaining water in the extract; 25 mg of primary secondary amine (PSA) to eliminate the high concentrations of sugars, organic acids, or fatty acids contained in the sample, and 2.5 mg of graphitized carbon black (GCB) to remove the elevated levels of pigments. The tube was shaken by vortexing for 30 s and centrifuged at 1500 rpm for 1 min [42]. Subsequently, the sample was concentrated using nitrogen flow to near-complete dryness, after which 1 mL of isooctane was added to the sample. Before being placed in vials, 25 µL and 100 µL of internal standards (PCB155 and PCB198) were added to the cell pellets to facilitate the analysis of the peaks by gas chromatography with an electron capture detector (GC-ECD, Hewlett Packard 6890 Series GC gas chromatograph equipped with 63Ni-ECD, using a fused silica CP-Sil 8 CB column (60 m length, diameter 0.25 mm diameter, 0.1 µm film thickness), according to ISO 10382 [43]. Five standard solutions were prepared, each with a concentration between 2 ng mL^{-1} and 12 ng $mL^{-}1$ for the calibration curve. Sample quantification was performed using a GC-ECD (Hewlett Packard 6890 Series GC gas chromatograph equipped with 63Ni-ECD, using a fused silica CP-Sil 8 CB column (60 m length, diameter 0.25 mm diameter, 0.1 µm film thickness), and the operating conditions and peaks corresponding to PCB 153 were identified according to the corresponding retention time, as previously described [43]. To ensure the quality control of PCB 153, a blank sample of the procedure was prepared, and a fortified blank sample and duplicate samples were prepared. For the blank and fortified samples, only DE was added to the extraction cell, and in the case of the fortified blank, 100 µL of the fortified standard was added. Fortified samples were prepared to evaluate the quality of the experiments. The criterion for acceptance of the blank samples was that their concentrations should be lower than the limit of detection (LD) of the method. For recovery tests, the value should be between 70 % and 130 %. For duplicate tests, the relative difference between the results should be less than 19.5 %.

2.3. Diatom photophysiology

Prior to cell harvesting, 1 mL of each replicate culture was utilized for photochemical chlorophyll a fluorescence measurements employing pulse amplitude modulated (PAM) fluorometry (FluorPen FP100, Photo System Instruments, Brno, Czech Republic). For photochemical assessment, culture subsamples were subjected to dark adaptation for 15 minutes, and chlorophyll transient light curves were generated using the pre-programmed OJIP protocol. [44]. The derived parameters are listed in Table S1.

2.4. Pigment profiles

The cell pellets were homogenized with 100 % (v/v) cold acetone and sonicated to ensure cell disruption. Samples were extracted overnight at −20 °C to prevent pigment degradation [25]. After extraction, the samples were centrifuged at 4000 × *g* for 15 min at 4 °C, and the clear supernatant was scanned (350 nm to 750 nm, 0.5 nm steps) using a dual-beam UV-1603 spectrophotometer (Shimadzu, Kyoto, Japan). Absorbance spectral data were analyzed using a Gauss-Peak Spectra (GPS) fitting library in SigmaPlot Software, and pigment concentrations were derived using the algorithm developed by [45]. The xanthophyll de-epoxidation state (DES) was calculated as the ratio of diatoxanthin to diadinoxanthin.

2.5. Fatty acid profiles

Cell pellets were trans-esterified using a methanol-sulfuric acid solution (97.5:2.5, v/v) at 70 °C for 60 min, and the resulting fatty acid methyl esters (FAMEs) were extracted using petroleum ether and dried under N_2 stream in a dry bath at 30 °C [25,44]. After reconstitution with hexane, the FAMEs were analyzed using a gas chromatograph (GC-FID, Clarus590, PerkinElmer, EUA) under the previously described chromatographic conditions [25,44]. Fatty acids were identified by comparing the retention times obtained from a standard collection (Sigma-Aldrich). Chromatograms were analyzed by the peak surface method using TotalChrome Navigator software (PerkinElmer, EUA). Pentadecanoic acid (C15:0) was used as an internal standard. The double bond index (DBI) was calculated as follows (Eq. 2):

$$DBI = \frac{2 \times (\%monoenes + 2 \times \%dienes + 3 \times \%trienes + 4 \times \%tetraenes + 5 \times \%pentaenes)}{100} \quad (2)$$

2.6. Oxidative stress biomarkers

Soluble protein was extracted from cell pellets by sonication (1 min) in 50 mM sodium phosphate buffer (pH 7.6, supplemented with 0.1 mM Na-EDTA). To remove cell debris, the extracts were centrifuged at 10,000 × g for 10 min at 4 °C and the supernatant containing proteins was collected. Protein concentration was determined as previously described [46]. Catalase (CAT), ascorbate peroxidase (APx), and superoxide dismutase (SOD) activities in the protein extract were analyzed by spectrophotometry using specific substrates, as previously described [24,44]. Lipid peroxidation products (assessed as thiobarbituric acid reactive substances (TBARS)) were analyzed spectrophotometrically [24,44] by extracting an additional cell pellet with trichloroacetic acid (20 % m/v), followed by a reaction with thiobarbituric acid (0.5 % m/v), and expressed as MDA equivalents.

2.7. Statistical analysis

All statistical analyses were performed using R-Studio 1.4.1717. Bar plots were generated using the *ggplot2* package [47]. Non-parametric Kruskal–Wallis tests with Bonferroni *post-hoc* corrections were conducted using the *agricolae* package [48]. Spearman's correlation coefficients and significance were assessed using the *corrplot* package [49]. Spearman correlation coefficients ($R^2 > 0.75$ or $R^2 < 0.75$) and statistical significance ($p < 0.05$) were used as thresholds for generating volcano plots depicting the most relevant features significantly correlated with the externally applied PCB-153 dose and intracellular PCB-153 concentration. Partial least squares-discriminant analysis (PLS-DA) was used to evaluate the ability to successfully classify individuals according to PCB-153 exposure concentrations using each of the considered biochemical and biophysical traits. Three components derived from the k-1 rule were used, where k is the number of experimental classes. Analyses were conducted using the *Discriminer* package [50]. Network analysis was conducted using Spearman's correlation coefficients using the *Hmisc* package [51].

3. Results

3.1. PCB internalization and cell growth features

The intracellular PCB-153 concentration in diatom cells exhibited significant variation across all experimental treatments, demonstrating a pronounced increase in response to elevated exogenous concentrations of PCB-153. Notably, the highest intracellular concentration was observed in cells exposed to the maximum concentration tested (Fig. 1A). Concurrently, the evaluation of cell density growth kinetics during ecotoxicological investigation demonstrated a significant decrease in cellular density within 24 h of exposure to the contaminant (72 h), resulting in markedly reduced cell density values by the conclusion of the exposure period (Fig. 1B). Further examination of the

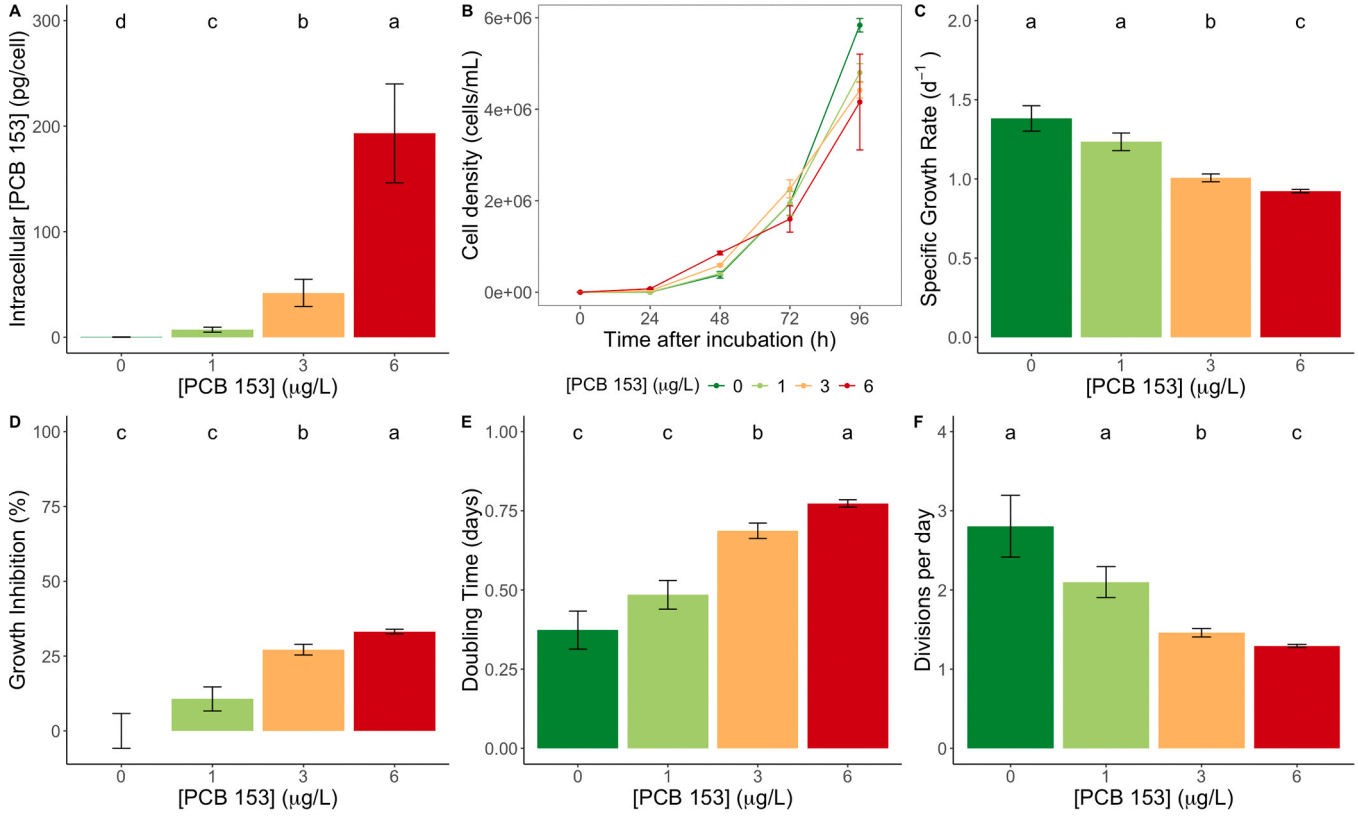

Fig. 1. PCB-153 intracellular accumulation (A) and growth features (B: cell density; C: specific growth rate; D: growth inhibition; E: doubling time; F: divisions per day) in *Phaeodactylum tricornutum* cells exposed to different PCB-153 concentrations test average ± standard error, N = 3; different letters denote significant changes at $p < 0.05$).

specific growth rates (Fig. 1C) revealed significantly reduced growth rates for diatom cultures exposed to 3 and 6 μg/L PCB-153, with the lowest rates recorded in cultures exposed to the maximum PCB concentration. This attenuation underscores the pronounced impediment in cellular proliferation due to increased PCB exposure, with maximal growth inhibition at 6 μg/L PCB-153. A calculated IC_{25} was possible to be achieved at 3.53 μg/L PCB-153. Considering the strong linear correlation between the exposed dose and the cell growth values measured within the range between 0 and 6 μg/L PCB-153, a predicted IC_{50} value of 7.09 μg/L PCB-153 could be derived, assuming a dose-response behavior similar to that reported within the range of tested concentrations. The No Observed Effect Concentration (NOEC) and the Lowest Observed Effect Concentration (LOEC) of 1 μg/L and 3 μg/L PCB-153, respectively, were determined. Concurrently, the doubling time significantly increased in cultures exposed to 3 and 6 μg/L PCB-153, with maximum elongation observed at the highest PCB exposure concentration. (Fig. 1E). Conversely, the rate of cellular division per day was significantly diminished following exposure to 3 μg/L and 6 μg/L, with the lowest division frequency observed in cultures exposed to 6 μg/L PCB-153 (Fig. 1F).

3.2. Diatom photochemical traits

The preliminary analysis of cellular photochemical characteristics utilizing Kautsky induction curves demonstrated significant alterations in the magnitude and morphology of the fluorescence profiles (Fig. 2). Specifically, cells exposed to higher concentrations of PCB-153 (3 and 6 μg/L) demonstrated reduced fluorescence across all curve phases, accompanied by curvilinear morphological alterations characterized by a loss of distinct inflection points.

Analysis of fluorescence induction signals yielded insights into cellular photochemical metabolism (Fig. 3). Exposure to PCB-153 significantly reduced the net rate of PSII RC closure compared with that in the controls (Fig. 3A). Cultures exposed to 3 μg/L and 6 μg/L PCB-153 demonstrated reduced oxidized quinone pool sizes, with the lowest values observed at the highest tested concentration. (Fig. 3B). The energy requirements for closing all RCs (Fig. 3C) and RC turnover rates (Fig. 3D) were significantly lower in cells exposed to 3 and 6 μg/L PCB-153. Grouping probability, indicative of PSII antenna disconnectivity, significantly increased with increasing PCB-153 concentration, peaking at 3 μg/L (Fig. 3E). Moreover, electron transport from PQH_2 to PSI end electron acceptors (Fig. 3F) and PSI acceptor-side electron acceptor reduction efficiency (Fig. 3G) were significantly higher in cells exposed to 3 μg/L and 6 μg/L PCB-153. Structural and functional indices of photochemical (Fig. 3H) and non-photochemical processes (Fig. 3I) exhibited significant alterations, particularly in cultures exposed to the highest tested PCB-153 concentration, characterized by decreased values in relation to photochemical reactions and concomitant increases with respect to non-photochemical reactions.

The energy fluxes governing photochemical processes demonstrated a significant reduction in absorbed, trapped, and transported energy fluxes with increasing PCB-153 exposure, with cultures exposed to 6 μg/L PCB-153 exhibiting a more pronounced decline (Fig. 4A). The dissipated energy flux also decreased in cells exposed to either 3 or 6 μg/L of PCB-153 (Fig. 4A). The number of active RC significantly decreased at all tested concentrations, exhibiting a gradient reduction corresponding to increasing PCB-153 concentration (Fig. 4A). Furthermore, a significant decrease in RC density across the PSII antenna chlorophyll bed was observed even in cells exposed to lower PCB-153 concentrations, with a more pronounced reduction in cultures subjected to PCB concentrations ranging from 3 to 6 μg/L (Fig. 4B).

3.3. Pigment and fatty acid profiles

Upon examination of chlorophyll *a, c,* and pheophytin *a* concentrations in cells exposed to 3 and 6 μg/L PCB-153, a significant increase in these pigments was observed in cultures subjected to these treatments (Fig. 5A). Beta-carotene and diadinoxanthin concentrations exhibited significant increases, particularly in the cultures exposed to 3 μg/L PCB-153 (Fig. 5A). Fucoxanthin concentration demonstrated a significant increase with increasing PCB-153 exposure, reaching its maximum in cells exposed to 6 μg/L PCB-153 (Fig. 5A). Diatoxanthin concentration was significantly elevated in cells exposed to 3 μg/L PCB-153 compared to other treatments (Fig. 5A). No significant alterations were observed in DES indices (Fig. 5B). The chlorophyll *a-to-c* ratio was significantly higher in cells exposed to 3 μg/L PCB-153 than in control cultures (Fig. 5C).

No statistically significant differences were observed in the individual fatty acid contents or classes (Fig. S1A), total content (Fig. S1B), or double bond index (DBI) parameters (Fig. S1C) among the various

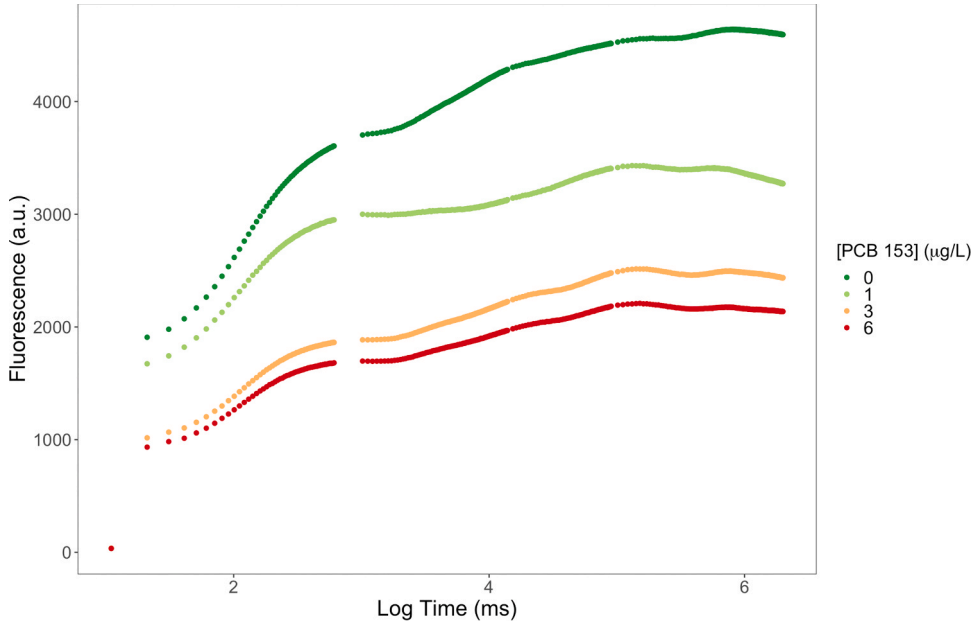

Fig. 2. Kautsky induction curve of *Phaeodactylum tricornutum* cells exposed to different PCB-153 concentrations (average, N = 3).

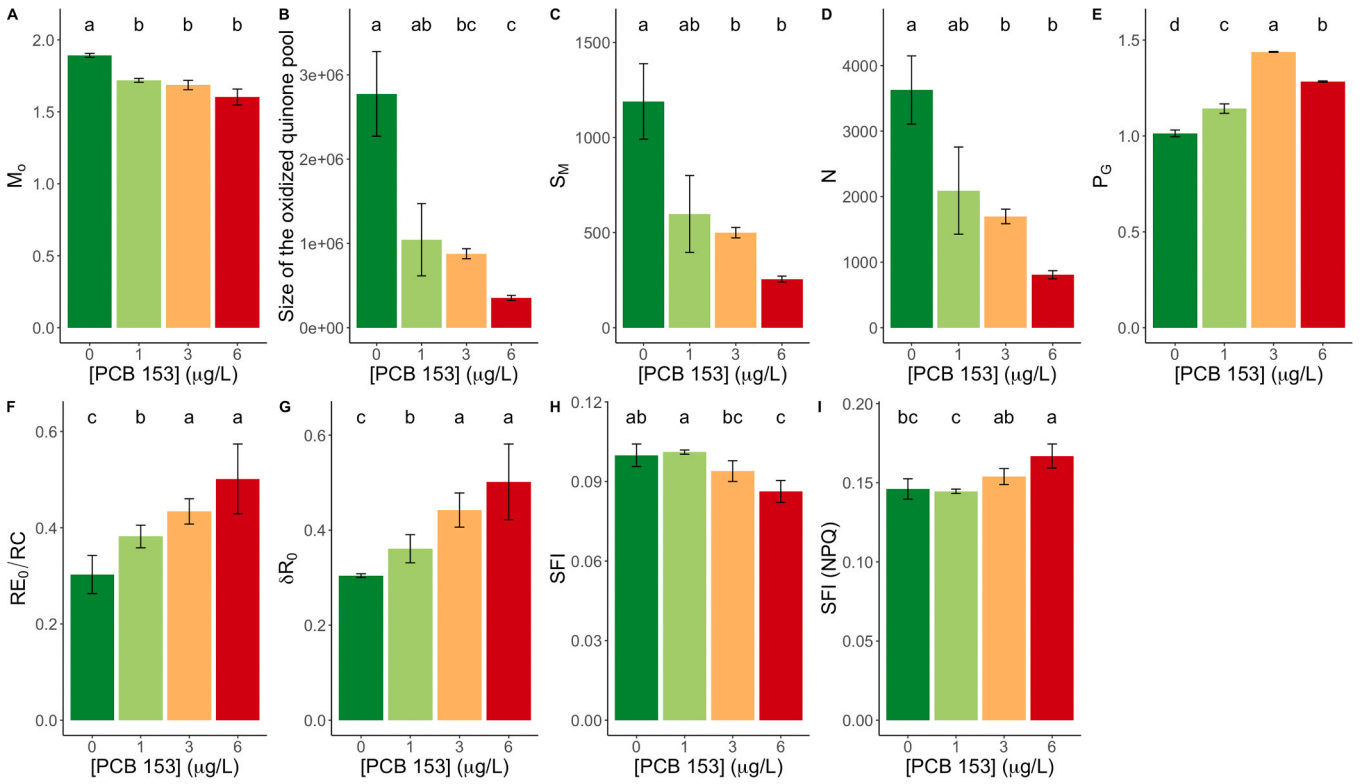

Fig. 3. The net rate of PSII reaction center (RC) closure (M_o, A), size of the oxidized quinone pool (B), energy needed to close all RC (S_M, C), RC turnover rate (N, D), grouping probability (P_G, E), electron transport from PQH_2 to the reduction of PSI end electron acceptors (RE_0/RC, F), PSI acceptor side end electron acceptor reduction efficiency (δR_0, G), structural and functional index of the photochemical (SFI, H) and non-photochemical [SFI(NPQ), I] reactions of *Phaeodactylum tricornutum* cells exposed to the different PCB-153 concentrations tested (average ± standard error, N = 3; different letters denote significant changes at $p < 0.05$).

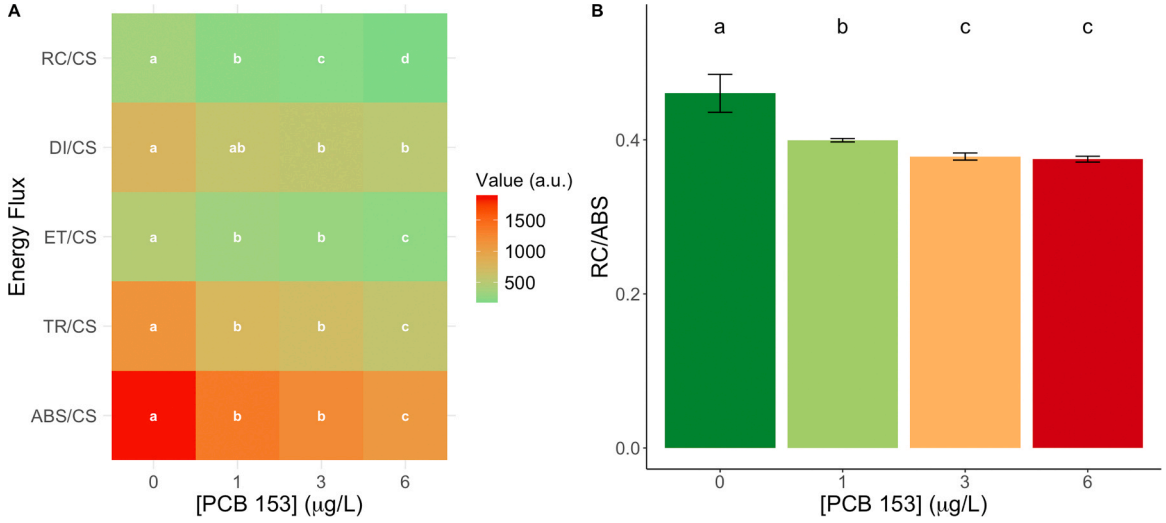

Fig. 4. Absorbed (ABS/CS), trapped (TR/CS), transported (ET/CS), and dissipated (DI/CS) energy fluxes, number of active reaction centers (RC) (RC/CS) heatmap (A), and RC density within the antenna chlorophyll bed of PSII (RC/ABS, B) of *Phaeodactylum tricornutum* cells exposed to different PCB-153 concentrations tested (average ± standard error, N = 3; different letters denote significant changes at $p < 0.05$).

treatments examined.

3.4. Oxidative stress biomarkers

The oxidative stress biomarkers examined (Fig. 6) exhibited increasing trends with elevated PCB-153 concentrations for all parameters. Catalase activity was significantly higher in cells exposed to 1 and 6 µg/L PCB-153 compared to the control (Fig. 6A). Ascorbate peroxidase activity reached its maximum in cells exposed to 6 µg/L of PCB-153 (Fig. 6B). The highest superoxide dismutase activity was observed in cells exposed to 1 and 6 µg/L PCB-153 (Fig. 6C). Moreover, lipid peroxidation products were elevated in cells exposed to PCB-153 compared to controls but demonstrated similar values across all exposure concentrations (Fig. 6D).

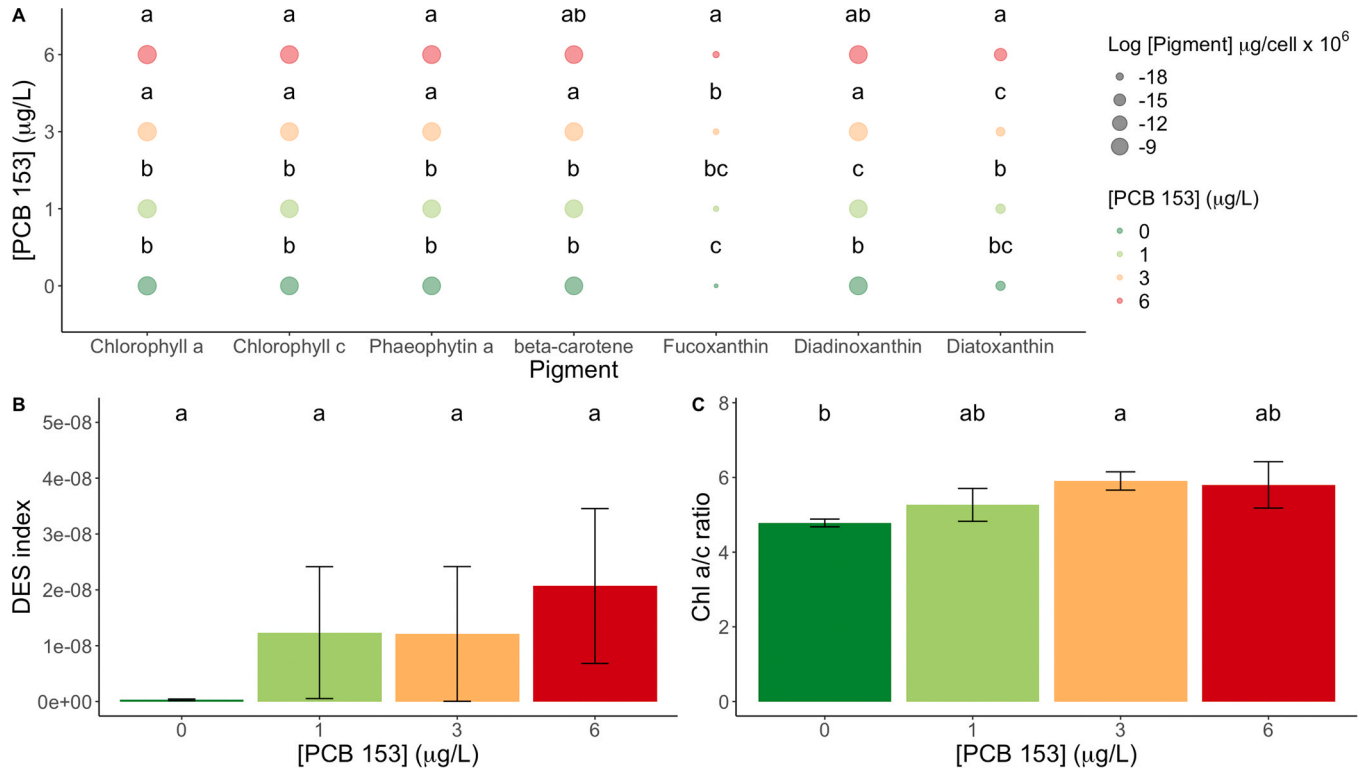

Fig. 5. Chlorophyll *a* and *c*, pheophytin *a*, carotenoid concentrations (A), the de-epoxidation state (DES) index (B), and chlorophyll *a* to *c* ratio (C) in *Phaeodactylum tricornutum* cells exposed to the different PCB-153 concentrations tested (average ± standard error, N = 3; different letters denote significant changes at $p < 0.05$).

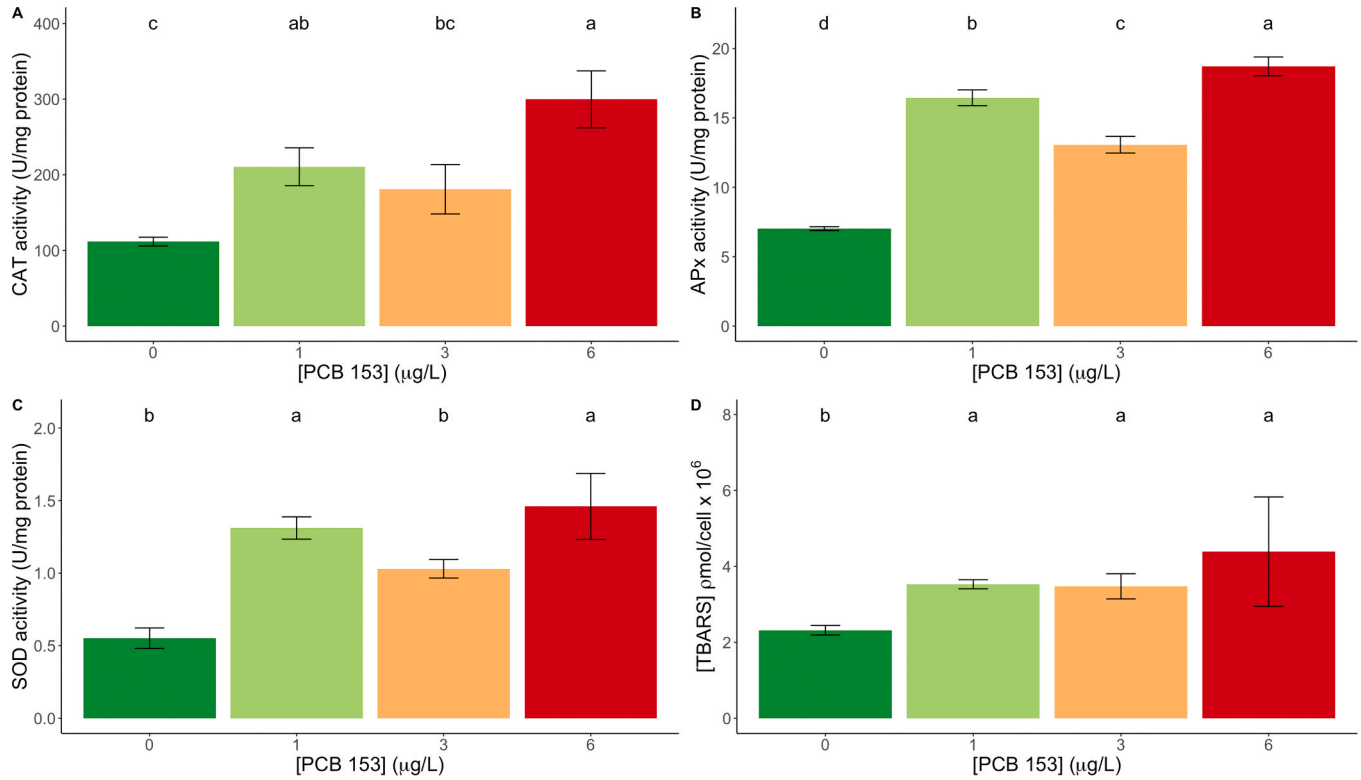

Fig. 6. Catalase (CAT) (A), ascorbate peroxidase (APx) (B), and superoxide dismutase (SOD) (C) activities and thiobarbituric acid reactive substances (TBARS) (D) in *Phaeodactylum tricornutum* cells exposed to the different PCB-153 concentrations tested (average ± standard error, N = 3; different letters denote significant changes at $p < 0.05$).

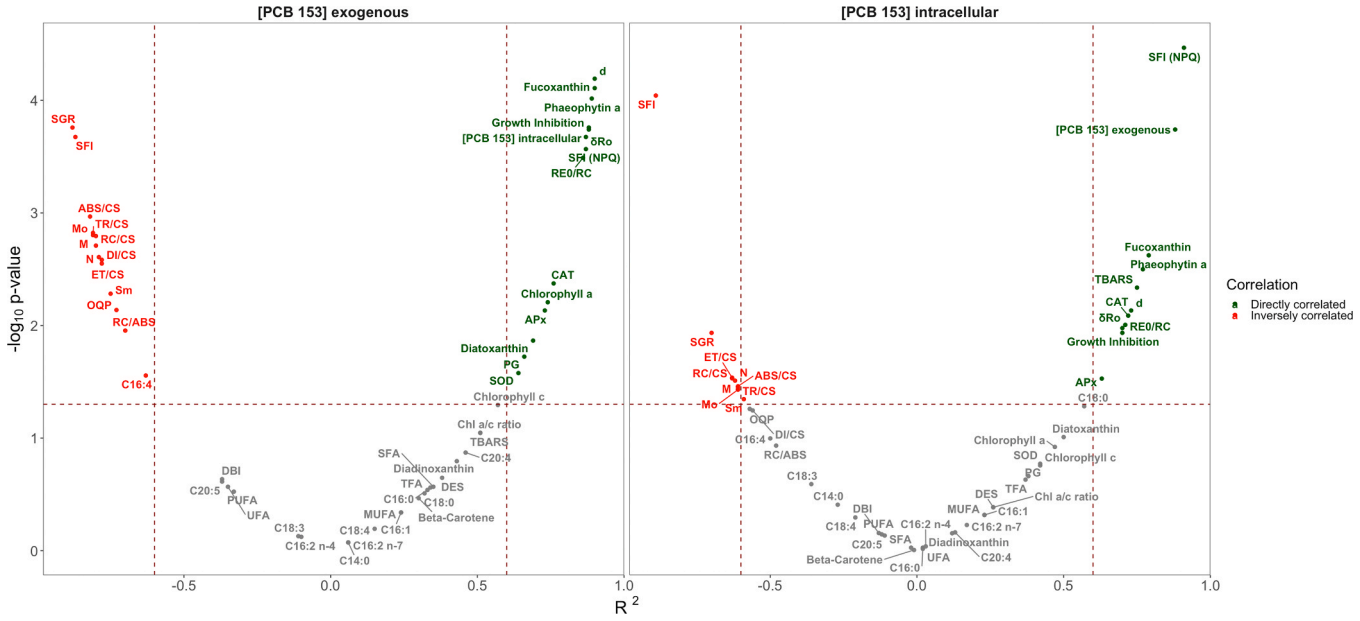

Fig. 7. Spearman volcano plots between the PCB-153 concentration applied exogenously and detected intracellularly and the growth parameters, photochemical traits, pigment concentrations, oxidative stress biomarkers, and fatty acid profiles of the *Phaeodactylum tricornutum* cells exposed to the different PCB-153 concentrations tested (horizontal dashed line indicates the $p < 0.05$, and vertical dashed lines indicate $R^2 = 0.75$ (right) and $R^2 = -0.75$ (left) thresholds, delimiting the highly significant and strong correlations).

3.5. *Dose-response relationships and multivariate classification*

Regarding dose-response relationships (Fig. 7), a clear correlation was observed between the intracellular concentration of PCB-153 and the applied exogenous dose. However, photochemical and biochemical traits exhibited distinct responses to exogenous or intracellular PCB-153 levels. Upon comparison of biomarkers to the nominal concentration of PCB-153 applied, 28 biomarkers demonstrated significant correlations: 14 were directly correlated and 14 were inversely correlated. In contrast, a smaller number of biomarkers exhibited significant dose-

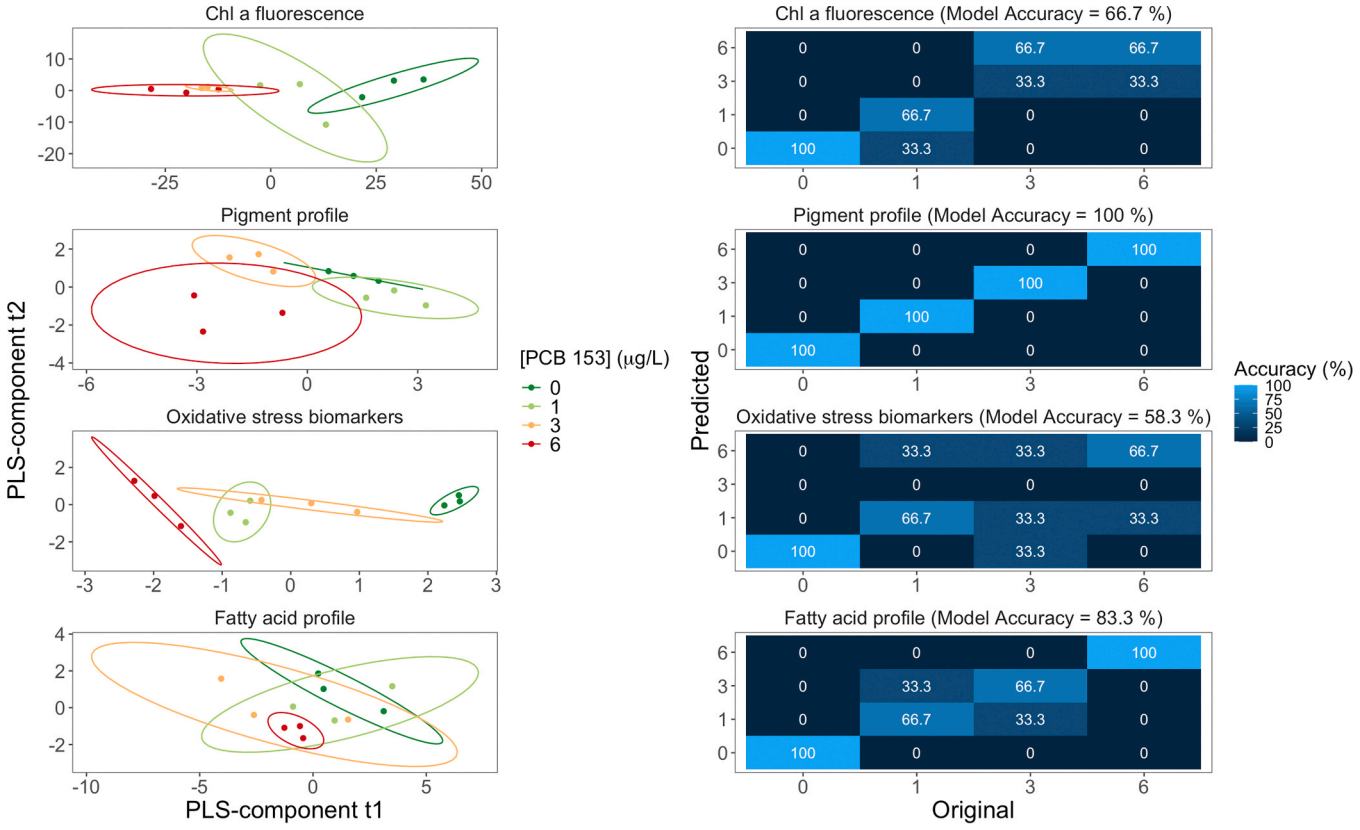

Fig. 8. Partial Least Square Discriminant Analysis (PLS-DA) biplots and confusion matrices relative to the photochemical, pigment, oxidative stress, and fatty acid traits measured in *Phaeodactylum tricornutum* cells exposed to the different PCB-153 concentrations tested.

response relationships with intracellular PCB-153 concentration: 11 traits demonstrated significant direct correlations, while 10 displayed inverse correlations. Notably, a high number of photochemical traits exhibited significant dose-response relationships with the nominal exogenous concentration, both directly and inversely. Regarding oxidative stress biomarkers, CAT, SOD, and APx activities exhibited strong correlations with the exogenous PCB-153 dose, whereas only APx and CAT activities demonstrated correlations with intracellular PCB-153 concentration. Growth inhibition and specific growth rate (SGR) were directly and inversely correlated, respectively, with both exogenous and intracellular PCB-153 levels. In the pigment profile, only fucoxanthin and phaeophytin *a* exhibited a significant correlation with intracellular PCB-153 concentrations. However, additional pigment profile traits had significant dose-response relationships when compared to the exogenous PCB-153 dose. Among the fatty acids examined, only the concentration of C16:4 exhibited a statistically significant relationship with PCB-153 exposure, demonstrating an inverse correlation with the administered dose.

The network analysis revealed that the complexity of the generated network (Fig. S2A) demonstrated a highly intricate biophysical and biochemical response with complex interrelationships. The majority of the edges (lines) connecting nodes (variables) were associated with photochemistry and pigment composition. Upon examination of the positive relationship network (Fig. S2B), several common responses were observed among the photochemical and pigment variables, as well as between these variables, fatty acid composition, and oxidative stress biomarkers. For example, Chlorophyll *a*, Chlorophyll *c*, and Diadinoxanthin appear to have a strong positive correlation with several variables, particularly those associated with fatty acids (e.g., C18:1 and C16:2) and biochemical stress markers (e.g., SOD and TBARS), indicating a common response of these metabolic segments. The majority of the inverse relationships observed among the analyzed variables were identified between pigment concentration-related variables and photochemical traits (Fig. S2C). Furthermore, CAT and APx exhibited a high number of edges with other variables, indicating an inverse relationship with numerous photochemical traits. The notably higher density of edges in the photochemical, oxidative stress, and pigment-related sectors underscores the centrality of these traits in the cellular response to PCB-153 exposure.

We employed a PLS-DA approach to assess the capacity of various datasets to differentiate between exposure groups and evaluate model accuracy (Fig. 8). Fluorescence data (raw Kautsky curve data to avoid co-variable interference) effectively differentiated experimental groups exposed to low PCB-153 concentrations, but exhibited high error rates for samples subjected to the highest concentrations, resulting in a model accuracy of 66.7 %. The pigment profile model based solely on individual pigment content demonstrated the highest classification accuracy (100 %) across all experimental groups. In contrast, the oxidative stress dataset exhibited the lowest classification accuracy (58.3 %), primarily due to misclassification of samples exposed to 3 μg/L PCB-153. However, classical univariate statistical analyses did not reveal any significant changes along the exposure gradient of the fatty acid profile, whereas models based on the fatty acid profile demonstrated high accuracy in detecting cells exposed to both the lowest and highest quantities and achieved moderate-to-high accuracy (66.7 %) for intermediate concentrations, yielding an overall model accuracy of 83.3 %.

4. Discussion

Previous research on the effects of PCBs on marine and freshwater phytoplankton has demonstrated their susceptibility to exposure to these contaminants. Early studies indicated that marine *Thalassiosira pseudonana* and *Skeletonema costatum* species exhibit reduced growth rates at PCB concentrations as low as 10–25 ppb, whereas freshwater and marine green algae species (*Dunaliella tertiolecta*) display resistance [52]. Differential sensitivities among freshwater algae have been attributed to PCB adsorption on glass surfaces and species-specific uptake properties rather than enzymatic degradation. [53]. A previous study targeting the green alga *Pseudokirchneriella subcapitata* demonstrated high toxicity of PCB 28, whereas PCBs 101 and 153 exhibited lower toxicity [54]. At the community level, marine phytoplankton isolates experienced temporary suppression of growth rate and photosynthesis at 10 μg/L PCB-153, with reduced chlorophyll *a* levels per cell and lower cell concentrations across all size classes [55]. In the present study, growth inhibition occurred at concentrations comparable to those previously reported, with severe effects observed at concentrations exceeding 3 μg/L, resulting in calculated IC_{25} and predicted IC_{50} values of 3.53 and 7.09 μg/L PCB-153 respectively, as well as a NOEC and a LOEC of 1 μg/L and 3 μg/L PCB-153, respectively. This growth inhibition was directly correlated with PCB-153 exposure dose and internalization in diatom cells, with cultures demonstrating a classical dose-response relationship. Research has indicated that PCB-153 can bioaccumulate in marine organisms, including diatoms [56]. In these phytoplankton species, PCB accumulation was observed to correlate with the degree of resistance exhibited by the strains, with lower accumulation noted in resistant strains compared to sensitive strains [56]. Additional research has demonstrated that light intensity is a critical factor influencing PCB-153 accumulation in diatoms, with higher light intensities resulting in increased toxicity and accumulation, thereby underscoring the interference of this compound in diatom photophysiology [57]. Our results are consistent with these findings (Table 1). Considering the previous half-maximal effective concentration for the tested PCB and other PCB compounds, the predicted IC_{50} results presented here are within the range observed for the same compound tested in *Selenastrum capricornutum* [58] and far below those observed for the remaining tested compounds, indicating a potentially higher toxicity of this compound when compared to other PCBs. However, it is important to note that there are also reports of half-maximal effective concentration values for PCB-153 significantly higher than those reported in this study [59,60], suggesting potential species-specific or culture-condition-specific effects of this compound. Furthermore, none of the previously reported studies have focused on the effects of marine diatoms, thus underscoring the necessity of the present investigation.

Although the mechanism of action of this compound in autotroph photochemistry remains unclear, our findings indicate its effects at multiple stages of the photochemical process. A severe reduction was observed in the number of available RCs for light harvesting on a cross-section and chlorophyll bed basis (as shown by RC/CS and RC/ABS, respectively), and in the functioning of these critical systems. More specifically, the rate at which the RCs were reduced upon illumination (M_o), the energy needed to reduce these systems (S_M), and their reoxidation rate (N) were severely reduced upon PCB-153 exposure. Moreover, the connectivity of the PSII antennae, which is crucial for light-energy harvesting, was reduced upon PCB-153 exposure, adding additional constraints to the light-harvesting process [62]. The reduction of

Table 1
Reported data on the ecotoxicity parameter EC_{50} (half maximal effective concentration) of PCB-153 and other PCB compounds in different marine algae.

Compound	Species used	EC_{50}	Reference
PCB−153	*Pseudokirchneriella subcapitata*	36.088 mg/L	[60]
PCB−153	*Tetraselmis suecica*	3.96 mg/L	[59]
PCB−153	*Selenastrum capricornutum*	0.0051 mg/L - 0.0866 mg/L	[58]
PCB−153	*Pseudokirchneriella subcapitata*	0.05–0.6 mg/L	[61]
PCB−153	*Scenedesmus obliquus*	~0.25 mg/L	[61]
PCB−31	*Selenastrum capricornutum*	78.6 mg/L	[58]
PCB−48	*Selenastrum capricornutum*	48.3 mg/L	[58]
PCB−105	*Selenastrum capricornutum*	5.47 mg/L	[58]
PCB−153	*Phaeodactylum tricornutum*	7.09 μg/L	This study

both available RC abundance and functioning inevitably diminishes the capacity of diatoms to harvest photons and convert their energy into electron potential (TR/CS). This phenomenon was accompanied by a reduced efficiency in utilizing the harvested energy for the production of chemical energy throughout the electron transport chain (ETC) in PCB-153-exposed diatoms. This is confirmed by the reduced size of the oxidized quinone pool available to transport the generated electrons, leading to a reduced electron transport energy flux and consequently impairing the electron transport from PQH_2 to the reduction of PSI end electron acceptors (RE_0/RC), and reducing the PSI acceptor side end electron acceptor reduction efficiency (δR_0). In contrast to observations in diatoms exposed to other organic contaminants [25,26], the proportional decrease in the absorbed and dissipated energy flux suggests a reduction in the light-harvesting process with subsequent proportional effects on photochemical events, rather than an inability to utilize the harvested energy.

This evidence suggests a direct influence of PCB-153 on PSII subunits and RC complexes, with subsequent indirect effects on the ETC, in contrast to the typically observed direct effects of exposure to organic contaminants on the diatom ETC [27,44]. Given its anchoring within a membrane system, any direct effect on the electron transport chain (ETC) following contaminant exposure is typically associated with alterations in diatom fatty acid profiles [28,63]. However, the exposed diatoms exhibited no significant differences at the individual fatty acid level, indicating that none of these compounds were directly affected by PCB-153 exposure, including those within the diatom thylakoid membrane. Among the fatty acids, only C16:4 concentration demonstrated a significant relationship to PCB-153 exposure, displaying an inverse correlation with the applied dose. This fatty acid is exclusively present in plastidial lipids, predominantly in monogalactosildiacylglycerol (MGDG), which constitutes the majority of thylakoid lipids [37]. This finding reinforces the hypothesis that PCB-153 directly affects the PSII complex rather than its peripheral photochemical components.

The increase in lipid peroxidation products (TBARS) was observed exclusively at lower PCB-153 concentrations, and their unaltered maintenance at higher levels corroborates not only the diminished effect of PCB-153 on the fatty acid profiles (particularly unsaturated ones) but also the potential activation of reactive oxygen species (ROS) buffer mechanisms even at exceedingly low PCB-153 concentrations. Previous studies have indicated that exposure to PCB-153 activates oxidative stress mechanisms in autotrophic organisms, which is inherently associated with decreased photosynthetic efficiency and enhanced expression or accumulation of transcripts (mRNA) of SOD genes [64,65]. Our results indicate proficient activation of the antioxidant enzymatic system at PCB-153 concentrations above 1 μg/L, efficiently quenching the generated ROS and preventing lipid peroxidation at the electron transport chain level. This observation aligns with the established susceptibility of Photosystem II (PSII) proteins to oxidative stress induced by reactive oxygen species (ROS) generated during photosynthesis [66], particularly the D1 protein in the PSII RC [67]. Moreover, PSII protein components are known to be more prone to oxidative stress than membrane ETC [68]. These findings support the hypothesis that the primary mechanism of toxicity is the direct impact of PCB-153 on the PSII complexes and their associated protein subunits.

Additional evidence supporting this mechanism can be observed through the analysis of diatom pigment composition upon PCB-153 exposure. Cultures exposed to higher PCB-153 concentrations showed increased cellular concentrations of chlorophyll *a* and its degradation product, pheophytin *a*. The latter is formed by the loss of the Mg atom in the center of the chlorophyll *a* molecule, which is typically associated with acidic conditions or oxidative stress [69]. Tetrapyrroles, including pheophytin, may result from oxidative stress-induced chlorophyll *a* degradation or tetrapyrrole-dependent mitigation of ROS generation and/or accumulation because their heme structure exhibits intrinsic peroxidase activity, making them important cofactors in ROS-detoxifying enzymes, including catalases and superoxide dismutases [69].

Another significant observation in the diatom pigment profile is the fucoxanthin cellular concentration, which demonstrated a marked increase along the PCB-153 exposure gradient. Research has indicated that fucoxanthin mitigates reactive oxygen species (ROS) generation, reduces lipid peroxidation, and enhances antioxidant levels in cells subjected to oxidative stress [70,71], including in marine diatoms [72]. Unlike many carotenoids, fucoxanthin functions beyond photoprotection and plays a vital role in light harvesting as part of fucoxanthin-chlorophyll proteins (FCPs) in diatoms [73]. Fucoxanthin efficiently transfers excitation energy to chlorophyll *a*, the main light-harvesting pigment [74]. Although FCPs are involved in both PSI and PSII, specific FCP subsets have been identified for each photosystem. In *Cyclotella meneghiniana*, FCPa associates with PSII, whereas a distinct FCP complex binds tightly to PSI [75]. These FCP photosystem supercomplexes facilitate efficient energy transfer, with fucoxanthin playing a key role in light harvesting [76,77]. The results obtained from the PCB-153-exposed diatoms indicate that the increase in fucoxanthin cellular concentration, concurrent with the decrease in PSII efficiency, suggests a negative feedback mechanism. This mechanism appears to maintain light-harvesting capacity while simultaneously enhancing PSII protection against oxidative stress, thereby enabling the cells to preserve a degree of photosynthetic efficiency even at higher PCB-153 concentrations examined.

Although PCB-153 exposure resulted in a complex network of events, as demonstrated by the network analysis (Supplementary Fig. S2), the primary events and consequences underlying the observed adverse outcomes can be summarized for enhanced comprehension (Fig. 9). In summary, PCB-153 exposure directly affects PSII reaction centers, impairing their capacity to capture and process light energy. This leads to a reduction in RC density and PSII antennae connectivity, ultimately impacting the light-harvesting capacity. Exposure to this compound also diminishes the ability to convert captured light into chemical energy (electron potential) and electron transport due to impaired quinone pool oxidation and lower reoxidation rates. This results in an accumulation of redox potential and the generation of reactive oxygen species (ROS), causing oxidative damage. The activation of antioxidant enzymes, such as SOD and CAT, allows, to a certain extent, the quenching of ROS. This was facilitated by an increase in Fucoxanthin concentration, which also mitigated the decreased light-harvesting efficiency. Nevertheless, ROS are not completely quenched, and Chlorophyll a degrades into Pheophytin a, accompanied by an increase in lipid peroxidation products resulting from cellular and plastidial membrane damage, which also has inevitable consequences for thylakoid photochemical processes.

In addition to elucidating the mechanism of action and endpoint effects of PCB-153, it is imperative to ascertain whether these physiological alterations can be utilized as effective indicators of its toxicity. Using a multivariate approach, the diatom pigment profiles proved to be a more efficient dataset for distinguishing different experimental exposure groups. Although no significant univariate differences were found in the diatom fatty acid profile, the subtle changes observed in intricate fatty acid metabolism revealed a high sensitivity in depicting the experimental exposure groups. This observation aligns with previous findings regarding the impact of various organic and inorganic contaminants on marine diatoms, underscoring the utility of a comprehensive analysis of diatom fatty acid profiles for detecting subtle alterations in ecotoxicity assessments [28]. The Kautsky curve and oxidative stress biomarker datasets exhibited the lowest integrated multivariate capacity to differentiate experimental PCB-153 exposure groups. Nevertheless, using a classical dose-response linear approach, several biomarkers were identified by comparing the responses of different parameters to the exogenous PCB-153 dose applied, as well as with the internalized concentration of this non-dioxin-like PCB. Several of the evaluated traits exhibited a consistent pattern when compared with exposure and measured PCB-153 cellular concentrations. Specifically, pheophytin *a*, fucoxanthin, catalase activity, SFI (NPQ), and

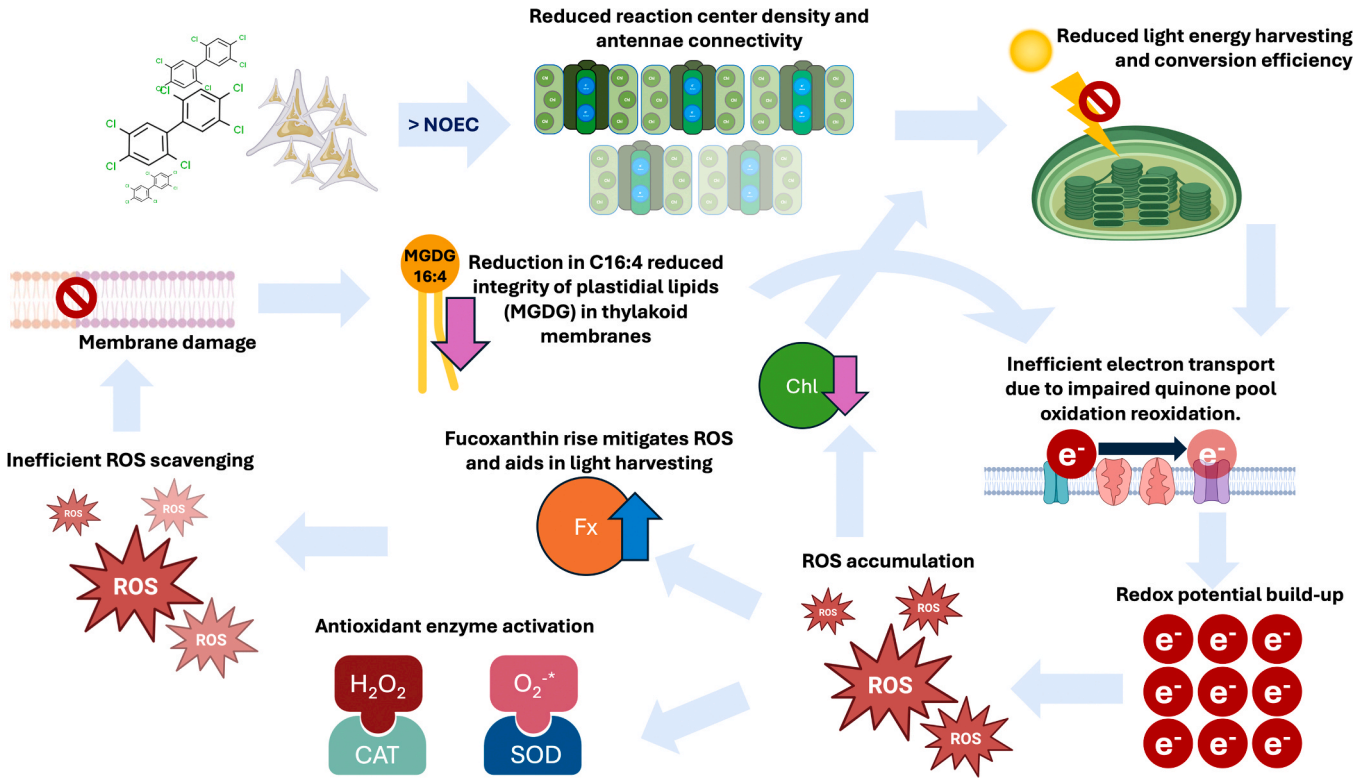

Fig. 9. Schematic representation of the main chain of events and consequences triggered by PCB-153 exposure in *Phaeodactylum tricornutum*.

classical growth inhibition emerged as the most appropriate directly related biomarkers for PCB-153 dose application and internalization. These findings are consistent with the mode-of-action hypothesis discussed above. Conversely, parameters related to PSII RC functioning (ABS/CS, ET/CS, TR/CS, S_M, and M_o), SFI, and the classical specific growth rate exhibited a strong inverse correlation with the applied and internalized PCB-153 dose, indicating potential biomarkers. Furthermore, this set of inversely correlated biomarkers corroborates the proposed PCB-153 mode of action hypothesis, substantiating their utility for ecotoxicological assessments and elucidating their metabolic and physiological effects in marine diatoms.

5. Conclusions

Non-dioxin-like PCB-153 induces severe impairment of marine diatom growth, even at very low concentrations, affecting key physiological processes. The observed toxicity is likely associated with direct effects on the functionality and abundance of PSII active RCs in marine diatoms, as they exhibit high sensitivity to oxidative stress induced by PCB-153 exposure. This impairment of PSII initiates cascading effects on the energy transduction pathway and chemical energy production system within these abundant marine primary producers, potentially significantly impacting ocean productivity and oxygen production. By affecting the base of the marine food web, exposure to this pollutant may potentially influence species at higher trophic levels, leading to alterations in the structure and function of marine communities and inevitably affecting the overall health of the marine ecosystem. Beyond these ecological consequences, the physiological impacts of PCB-153 on diatoms have also facilitated the identification of an efficient and reliable set of biomarkers for future ecotoxicological assessments, providing sensitive responses even at low environmentally relevant concentrations. These biomarkers demonstrate significant potential for informing environmental monitoring programs and guiding policy-making efforts aimed at mitigating the impact of these persistent contaminants in marine systems.

Environmental implication

Despite the worldwide ban on PCBs, the congener 153 (PCB-153, 2, 2′, 4, 4′, 5, 5′–hexachlorobiphenyl) is still detected at significant concentrations in biotic and abiotic compartments, with reported toxic effects in several organisms. Nevertheless, despite its evaluation in several model organisms, the effects and mode of action of PCB-153 on the major marine phytoplankton group, diatoms, remain largely unknown. Considering this knowledge gap, it is of utmost importance to depict these mechanisms while extracting potential effect biomarkers of diatom exposure to PCB-153 for future ecotoxicological assessments, ultimately aiding in mitigating its environmental impacts.

CRediT authorship contribution statement

Feijão Eduardo: Writing – review & editing, Methodology, Investigation. **Carreiras João Albuquerque:** Writing – review & editing, Methodology, Investigation. **Cardoso João:** Writing – original draft, Methodology, Investigation, Formal analysis. **Fonseca Vanessa:** Writing – review & editing. **Santos Paula:** Writing – review & editing, Methodology, Investigation, Data curation. **de Carvalho Ricardo Cruz:** Writing – review & editing, Methodology, Investigation. **Matos Ana:** Writing – review & editing. **Duarte Bernardo:** Writing – original draft, Supervision, Resources, Project administration, Funding acquisition, Formal analysis, Data curation, Conceptualization. **Palma Carla:** Writing – review & editing, Supervision, Resources, Project administration, Funding acquisition, Data curation, Conceptualization.

Declaration of Competing Interest

The authors declare that they have no known competing financial interests or personal relationships that could have appeared to influence the work reported in this paper.

Acknowledgements

The authors would like to thank Fundação para a Ciência e a Tecnologia (FCT) for funding MARE (Marine and Environmental Sciences Centre, http://doi.org/10.54499/UIDB/04292/2020 and http://doi.org/10.54499/UIDP/04292/2020), ARNET (Aquatic Research Network Associated Laboratory, http://doi.org/10.54499/LA/P/0069/2020), BioISI (Biosystems and Integrative Sciences Institute, http://doi.org/10.54499/UIDB/04046/2020 and http://doi.org/10.54499/UIDP/04046/2020), Ce3C (Centre for Ecology, Evolution and Environmental Changes, http://doi.org/10.54499/UIDB/00329/2020 and http://doi.org/10.54499/UIDP/00329/2020) and CHANGE (Global Change and Sustainability Institute, http://doi.org/10.54499/LA/P/0121/2020). E. Feijão and J. Carreiras were supported by FCT Ph.D. Grants (2022.11916.BD and 2022.11260.BD respectively).

Appendix A. Supporting information

Supplementary data associated with this article can be found in the online version at doi:10.1016/j.jhazmat.2025.137653.

Data availability

Data will be made available on request.

References

[1] Grilo, T.F., Cardoso, P.G., Pato, P., Duarte, A.C., Pardal, M.A., 2014. Uptake and depuration of PCB-153 in edible shrimp Palaemonetes varians and human health risk assessment. Ecotoxicol Environ Saf 101, 97–102. https://doi.org/10.1016/j.ecoenv.2013.12.020.

[2] Nakari, T., Huhtala, S., 2008. Comparison of toxicity of congener-153 of PCB, PBB, and PBDE to Daphnia magna. Ecotoxicol Environ Saf 71, 514–518. https://doi.org/10.1016/j.ecoenv.2007.10.012.

[3] Abass, K., Huusko, A., Nieminen, P., Myllynen, P., Pelkonen, O., Vahakangas, K., et al., 2013. Estimation of health risk by using toxicokinetic modelling: a case study of polychlorinated biphenyl PCB153. J Hazard Mater 261, 1–10. https://doi.org/10.1016/j.jhazmat.2013.07.011.

[4] De, S., Pramanik, S.K., Williams, A.L., Dutta, S.K., 2004. Toxicity of polychlorobiphenyls and its bioremediation. Int J Hum Genet 4, 281–290. https://doi.org/10.1080/09723757.2004.11885907.

[5] Weisglas-Kuperus, N., 1998. Neurodevelopmental, immunological and endocrinological indices of perinatal human exposure to PCBs and dioxins. Chemosphere 37, 1845–1853. https://doi.org/10.1016/S0045-6535(98)00250-1.

[6] Corsolini, S., Sarà, G., 2017. The trophic transfer of persistent pollutants (HCB, DDTs, PCBs) within polar marine food webs. Chemosphere 177, 189–199. https://doi.org/10.1016/j.chemosphere.2017.02.116.

[7] Eisler, R., 2000. Handbook of Chemical Risk Assessment: Health Hazards to Humans, Plants, and Animals, Three Volume Set. CRC Press. https://doi.org/10.1201/9781420032741.

[8] Carro, N., García, I., Ignacio, M., Mouteira, A., 2002. Levels and distribution patterns of polychlorinated biphenyl congeners in surface sediments from galicia coast (North-Western, Spain) according to granulometric characteristics. Environ Technol 23, 919–930. https://doi.org/10.1080/09593332308618362.

[9] Geyer, H., Freitag, D., Korte, F., 1984. Polychlorinated biphenyls (PCBs) in the marine environment, particularly in the mediterranean. Ecotoxicol Environ Saf 8, 129–151. https://doi.org/10.1016/0147-6513(84)90056-3.

[10] Agbo, I.A., Abaye, D., 2016. Levels of polychlorinated biphenyls in plastic resin pellets from six beaches on the accra-tema coastline, Ghana. J Health Pollut 6, 9–17. https://doi.org/10.5696/2156-9614-6-11.9.

[11] Abarnou, A., Avoine, J., Dupont, J.P., Lafite, R., Simon, S., 1987. Role of suspended sediments on the distribution of PCB in the Seine Estuary (France). Cont Shelf Res 7, 1345–1350. https://doi.org/10.1016/0278-4343(87)90038-0.

[12] Chu, S., Covaci, A., Schepens, P., 2003. Levels and chiral signatures of persistent organochlorine pollutants in human tissues from Belgium. Environ Res 93, 167–176. https://doi.org/10.1016/S0013-9351(03)00016-1.

[13] Honkakoski, P., Sueyoshi, T., Negishi, M., 2003. Drug-activated nuclear receptors CAR and PXR. Ann Med 35, 172–182. https://doi.org/10.1080/07853890310008224.

[14] Al-Salman, F., Plant, N., 2012. Non-coplanar polychlorinated biphenyls (PCBs) are direct agonists for the human pregnane-X receptor and constitutive androstane receptor, and activate target gene expression in a tissue-specific manner. Toxicol Appl Pharmacol 263, 7–13. https://doi.org/10.1016/j.taap.2012.05.016.

[15] Halm-Lemeille, M.-P., Abbaszadeh Fard, E., Latire, T., Ferard, J.-F., Costil, K., Lebel, J.-M., et al., 2014. The effect of different polychlorinated biphenyls on two aquatic models, the green alga Pseudokirchneriella subcapitata and the haemocytes from the European abalone Haliotis tuberculata. Chemosphere 110, 120–128. https://doi.org/10.1016/j.chemosphere.2014.02.023.

[16] Mayer, P., Halling-Sørensen, B., Sijm, D.T.H.M., Nyholm, N., 1998. Toxic cell concentrations of three polychlorinated biphenyl congeners in the green alga Selenastrum capricornutum. Environ Toxic Chem 17, 1848–1851. https://doi.org/10.1002/etc.5620170927.

[17] Malviya, S., Scalco, E., Audic, S., Vincent, F., Veluchamy, A., Poulain, J., et al., 2016. Insights into global diatom distribution and diversity in the world's ocean. Proc Natl Acad Sci 113, E1516–E1525. https://doi.org/10.1073/pnas.1509523113.

[18] Domingues, N., Matos, A.R., da Silva, J.M., Cartaxana, P., 2012. Response of the Diatom Phaeodactylum tricornutum to photooxidative stress resulting from high light exposure. PLoS ONE 7 (6), 1. https://doi.org/10.1371/journal.pone.0038162.

[19] Benoiston, A.-S., Ibarbalz, F.M., Bittner, L., Guidi, L., Jahn, O., Dutkiewicz, S., et al., 2017. The evolution of diatoms and their biogeochemical functions. Philos Trans R Soc B Biol Sci 372, 20160397. https://doi.org/10.1098/rstb.2016.0397.

[20] Renzi, M., Roselli, L., Giovani, A., Focardi, S.E., Basset, A., 2014. Early warning tools for ecotoxicity assessment based on Phaeodactylum tricornutum. Ecotoxicology 23, 1055–1072. https://doi.org/10.1007/s10646-014-1249-z.

[21] Duarte, B., Feijão, E., Cruz de Carvalho, R., Franzitta, M., Carlos Marques, J., Caçador, I., et al., 2021. Unlocking Kautsky's dark box: development of an optical toxicity classification tool (OPTOX index) with marine diatoms exposed to emerging contaminants. Ecol Indic 131, 108238. https://doi.org/10.1016/j.ecolind.2021.108238.

[22] Cabrita, M.T., Gameiro, C., Utkin, A.B., Duarte, B., Caçador, I., Cartaxana, P., 2016. Photosynthetic pigment laser-induced fluorescence indicators for the detection of changes associated with trace element stress in the diatom model species Phaeodactylum tricornutum. Environ Monit Assess 188, 285. https://doi.org/10.1007/s10661-016-5293-4.

[23] Utkin, A.B., Duarte, B., Cabrita, M.T., 2020. Prospective of laser-induced fluorescence as a non-invasive tool for ecotoxicological assessments. In: Proc. - Int. Conf. Laser Opt. ICLO, Institute of Electrical and Electronics Engineers Inc. https://doi.org/10.1109/ICLO48556.2020.9285763

[24] Pires, V.L., Novais, S.C., Lemos, M.F.L., Fonseca, V.F., Duarte, B., 2021. Evaluation of multivariate biomarker indexes application in ecotoxicity tests with marine diatoms exposed to emerging contaminants. BIOLOGY. https://doi.org/10.20944/preprints202103.0735.v1.

[25] Feijão, E., Cruz de Carvalho, R., Duarte, I.A., Matos, A.R., Cabrita, M.T., Novais, S.C., et al., 2020. Fluoxetine arrests growth of the model diatom phaeodactylum tricornutum by increasing oxidative stress and altering energetic and lipid metabolism. Front Microbiol 11, 1803. https://doi.org/10.3389/fmicb.2020.01803.

[26] Cruz de Carvalho, R., Feijão, E., Matos, A.R., Cabrita, M.T., Novais, S.C., Lemos, M.F.L., et al., 2020. Glyphosate-based herbicide toxicophenomics in marine diatoms: impacts on primary production and physiological fitness. Appl Sci 10, 1–21. https://doi.org/10.3390/app10217391.

[27] Duarte, B., Feijão, E., Cruz de Carvalho, R., Matos, A.R., Cabrita, M.T., Novais, S.C., et al., 2022. Effect biomarkers of the widespread antimicrobial triclosan in a marine model diatom. Antioxidants 11. https://doi.org/10.3390/antiox11081442.

[28] Duarte, B., Feijão, E., Franzitta, M., Duarte, I.A., de Carvalho, R.C., Cabrita, M.T., et al., 2022. LipidTOX: a fatty acid-based index efficient for ecotoxicological studies with marine model diatoms exposed to legacy and emerging contaminants. Ecol Indic 139, 108885. https://doi.org/10.1016/j.ecolind.2022.108885.

[29] Duarte, B., Feijão, E., Cruz de Carvalho, R., Duarte, I.A., Marques, A.P., Maia, M., et al., 2022. Untargeted metabolomics reveals antidepressant effects in a marine photosynthetic organism: the diatom phaeodactylum tricornutum as a case study. Biology 11, 1770. https://doi.org/10.3390/biology11121770.

[30] Renzi, M., Roselli, L., Giovani, A., Focardi, S.E., Basset, A., 2014. Early warning tools for ecotoxicity assessment based on Phaeodactylum tricornutum. Ecotoxicology 23, 1055–1072. https://doi.org/10.1007/s10646-014-1249-z.

[31] Moreira-Santos, M., Soares, A.M.V.M., Ribeiro, R., 2004. A phytoplankton growth assay for routine in situ environmental assessments. Environ Toxic Chem 23, 1549–1560. https://doi.org/10.1897/03-389.

[32] De Martino, A., Bartual, A., Willis, A., Meichenin, A., Villazán, B., Maheswari, U., et al., 2011. Physiological and molecular evidence that environmental changes elicit morphological interconversion in the model diatom phaeodactylum tricornutum. Protist 162, 462–481. https://doi.org/10.1016/j.protis.2011.02.002.

[33] Francius, G., Tesson, B., Dague, E., Martin-Jézéquel, V., Dufrêne, Y.F., 2008. Nanostructure and nanomechanics of live Phaeodactylum tricornutum morphotypes. Environ Microbiol 10, 1344–1356. https://doi.org/10.1111/j.1462-2920.2007.01551.x.

[34] Falasco, E., Bona, F., Badino, G., Hoffmann, L., Ector, L., 2009. Diatom teratological forms and environmental alterations: a review. Hydrobiologia 623, 1–35. https://doi.org/10.1007/s10750-008-9687-3.

[35] Othman, H.B., Leboulanger, C., Le Floc'h, E., Hadj Mabrouk, H., Sakka Hlaili, A., 2012. Toxicity of benz(a)anthracene and fluoranthene to marine phytoplankton in culture: does cell size really matter? J Hazard Mater 243, 204–211. https://doi.org/10.1016/j.jhazmat.2012.10.020.

[36] Guillard, R.R.L., Ryther, J.H., 1962. Studies of marine planktonic diatoms: I. CYCLOTELLA NANA HUSTEDT, AND Detonula confervacea (CLEVE) GRAN. Can J Microbiol 8, 229–239. https://doi.org/10.1139/m62-029.

[37] Feijão, E., Gameiro, C., Franzitta, M., Duarte, B., Caçador, I., Cabrita, M.T., et al., 2018. Heat wave impacts on the model diatom Phaeodactylum tricornutum: searching for photochemical and fatty acid biomarkers of thermal stress. Ecol Indic 95, 1026–1037. https://doi.org/10.1016/j.ecolind.2017.07.058.

[38] OECD, 2011. OECD Guidelines for the testing of Chemicals. Freshwater Alga and Cyanobacteria, Growth Inhibition Test. Organisation for Economic Cooperation and Development, pp. 1–25. https://doi.org/10.1787/9789264203785-en.
[39] Vlotman, D.E., Ngila, J.C., Ndlovu, T., Doyle, B., Carleschi, E., Malinga, S.P., 2019. Hyperbranched polymer membrane for catalytic degradation of polychlorinated biphenyl-153 (PCB-153) in water. React Funct Polym 136, 44–57. https://doi.org/10.1016/j.reactfunctpolym.2018.12.019.
[40] Cruz De Carvalho, R., Cardoso, J., Carreiras, J.A., Santos, P., Palma, C., Duarte, B., 2024. Persistent Organic pollutants in tagus estuary salt marshes: patterns of contamination and plant uptake. JoX 14, 1165–1186. https://doi.org/10.3390/jox14030066.
[41] Santos-Ballardo, D.U., Rossi, S., Hernández, V., Gómez, R.V., del Carmen Rendón-Unceta, M., Caro-Corrales, J., et al., 2015. A simple spectrophotometric method for biomass measurement of important microalgae species in aquaculture. Aquaculture 448, 87–92. https://doi.org/10.1016/j.aquaculture.2015.05.044.
[42] Lehotay, S.J., 2007. Determination of pesticide residues in foods by acetonitrile extraction and partitioning with magnesium sulfate: collaborative study. J AOAC Int 90, 485–520.
[43] ISO 10382, ISO 10382:2002(E) Soil Quality – Determination of Organochlorine Pesticides and Polychlorinated Bipheyls – Gas Chromatography Method with Electron Capture Detection, (2002).
[44] Duarte, B., Feijão, E., Cruz de Carvalho, R., Duarte, I.A., Silva, M., Matos, A.R., et al., 2020. Effects of propranolol on growth, lipids and energy metabolism and oxidative stress response of phaeodactylum tricornutum. Biology 9, 478. https://doi.org/10.3390/biology9120478.
[45] Küpper, H., Seibert, S., Parameswaran, A., 2007. Fast, sensitive, and inexpensive alternative to analytical pigment HPLC: quantification of chlorophylls and carotenoids in crude extracts by fitting with Gauss peak spectra. Anal Chem 79, 7611–7627. https://doi.org/10.1021/ac070236m.
[46] Bradford, M.M., 1976. A rapid and sensitive method for the quantitation of microgram quantities of protein utilizing the principle of protein-dye binding. Anal Biochem 72, 248–254. https://doi.org/10.1016/0003-2697(76)90527-3.
[47] Wickham, H., 2009. ggplot2: elegant graphics for data analysis. Springer-Verlag, New York. https://doi.org/10.1007/978-0-387-98141-3.
[48] Mendiburu, F.De, Simon, R., 2015. Agricolae - Ten years of an open source statistical tool for experiments in breeding. Agric Biol, (. https://doi.org/10.7287/peerj.preprints.1404v1.
[49] Taiyun, taiyun/corrplot, 2021. ⟨https://github.com/taiyun/corrplot/blob/e601361809c28242f8f16029a9a49923722d82b4/inst/CITATION⟩ (Accessed October 19, 2021).
[50] G. Sanchez, Package 'DiscriMiner,' 2013. ⟨https://www.gastonsanchez.com/discriminer⟩.
[51] F. Harrell Jr, Hmisc: Harrell Miscellaneous, 2025. ⟨https://github.com/harrelfe/hmisc⟩.
[52] Mosser, J.L., Fisher, N.S., Teng, T.-C., Wurster, C.F., 1972. Polychlorinated biphenyls: toxicity to certain phytoplankters. Science 175, 191–192. https://doi.org/10.1126/science.175.4018.191.
[53] Mahanty, H.K., Gresshoff, P.M., 1978. Influence of polychlorinated biphenyls (PCBs) on growth of freshwater algae. Bot Gaz 139, 202–206. https://doi.org/10.1086/336988.
[54] Halm-Lemeille, M.-P., Abbaszadeh Fard, E., Latire, T., Ferard, J.-F., Costil, K., Lebel, J.-M., et al., 2014. The effect of different polychlorinated biphenyls on two aquatic models, the green alga Pseudokirchneriella subcapitata and the haemocytes from the European abalone Haliotis tuberculata. Chemosphere 110, 120–128. https://doi.org/10.1016/j.chemosphere.2014.02.023.
[55] Powers, C.D., Rowland, R.G., O'Connors, H.B., Wurster, C.F., 1977. Response to polychlorinated biphenyls of marine phytoplankton isolates cultured under natural conditions. Appl Environ Microbiol 34, 760–764. https://doi.org/10.1128/aem.34.6.760-764.1977.
[56] Cohen, M.K., West, A.S., Cosper, E.M., Wurster, C.F., 1991. Mechanisms of resistance to polychlorinated biphenyls (PCB) in two species of marine diatoms. J Mar Biol Assess 71, 247–263. https://doi.org/10.1017/S0025315400051596.
[57] Ruben, H.J., Cosper, E.M., Wurster, C.F., 1990. Influence of light intensity and photoadaptation on the toxicity of PCB to a marine diatom. Environ Toxic Chem 9, 777–784. https://doi.org/10.1002/etc.5620090612.
[58] Mayer, P., Halling-Sørensen, B., Sijm, D.T.H.M., Nyholm, N., 1998. Toxic cell concentrations of three polychlorinated biphenyl congeners in the green alga Selenastrum capricornutum. Environ Toxicol Chem 17, 1848–1851. https://doi.org/10.1002/etc.5620170927.
[59] Ki, Jang-Seu, 2013. Quantification of the sub-lethal toxicity of metals and endocrine-disrupting chemicals to the Marine Green Microalga Tetraselmis suecica. Fish Aquat Sci 16, 187–194. https://doi.org/10.5657/FAS.2013.0187.
[60] Halm-Lemeille, M.-P., Abbaszadeh Fard, E., Latire, T., Ferard, J.-F., Costil, K., Lebel, J.-M., et al., 2014. The effect of different polychlorinated biphenyls on two aquatic models, the green alga Pseudokirchneriella subcapitata and the haemocytes from the European abalone Haliotis tuberculata. Chemosphere 110, 120–128. https://doi.org/10.1016/j.chemosphere.2014.02.023.
[61] Wang, Q., Yan, S., Chang, C., Qu, C., Tian, Y., Song, J., et al., 2023. Occurrence, potential risk assessment, and source apportionment of polychlorinated biphenyls in water from Beiluo river. Water 15, 459. https://doi.org/10.3390/w15030459.
[62] Kovács, L., Damkjær, J., Kereïche, S., Ilioaia, C., Ruban, A.V., Boekema, E.J., et al., 2006. Lack of the light-harvesting complex CP24 affects the structure and function of the grana membranes of higher plant chloroplasts. Plant Cell 18, 3106–3120. https://doi.org/10.1105/tpc.106.045641.
[63] González-Fernández, C., Le Grand, F., Bideau, A., Huvet, A., Paul-Pont, I., Soudant, P., 2020. Nanoplastics exposure modulate lipid and pigment compositions in diatoms. Environ Pollut 262, 114274. https://doi.org/10.1016/j.envpol.2020.114274.
[64] Ahammed, G.J., Ruan, Y.-P., Zhou, J., Xia, X.-J., Shi, K., Zhou, Y.-H., et al., 2013. Brassinosteroid alleviates polychlorinated biphenyls-induced oxidative stress by enhancing antioxidant enzymes activity in tomato. Chemosphere 90, 2645–2653. https://doi.org/10.1016/j.chemosphere.2012.11.041.
[65] Enayah, S.H., Vanle, B.C., Fuortes, L.J., Doorn, J.A., Ludewig, G., 2018. PCB95 and PCB153 change dopamine levels and turn-over in PC12 cells. Toxicology 394, 93–101. https://doi.org/10.1016/j.tox.2017.12.003.
[66] Pospíšil, P., 2012. Molecular mechanisms of production and scavenging of reactive oxygen species by photosystem II. Biochim Et Biophys Acta (BBA) - Bioenerg 1817, 218–231. https://doi.org/10.1016/j.bbabio.2011.05.017.
[67] Aro, E.-M., 2004. Dynamics of photosystem II: a proteomic approach to thylakoid protein complexes. J Exp Bot 56, 347–356. https://doi.org/10.1093/jxb/eri041.
[68] Pospíšil, P., Yamamoto, Y., 2017. Damage to photosystem II by lipid peroxidation products. Biochim Et Biophys Acta (BBA) - Gen Subj 1861, 457–466. https://doi.org/10.1016/j.bbagen.2016.10.005.
[69] Busch, A.W.U., Montgomery, B.L., 2015. Interdependence of tetrapyrrole metabolism, the generation of oxidative stress and the mitigative oxidative stress response. Redox Biol 4, 260–271. https://doi.org/10.1016/j.redox.2015.01.010.
[70] Chen, S.-J., Lin, T.-B., Peng, H.-Y., Liu, H.-J., Lee, A.-S., Lin, C.-H., et al., 2021. Cytoprotective potential of fucoxanthin in oxidative stress-induced age-related macular degeneration and retinal pigment epithelial cell senescence in vivo and in vitro. Mar Drugs 19, 114. https://doi.org/10.3390/md19020114.
[71] Liu, C.-L., Liang, A.-L., Hu, M.-L., 2011. Protective effects of fucoxanthin against ferric nitrilotriacetate-induced oxidative stress in murine hepatic BNL CL.2 cells. Toxicol Vitr 25, 1314–1319. https://doi.org/10.1016/j.tiv.2011.04.023.
[72] Erdogan, A., Demirel, Z., Dalay, M.C., Eroglu, A.E., 2016. Fucoxanthin content of cylindrotheca closterium and its oxidative stress mediated enhancement. Turk J Fish Aquat Sci 16. https://doi.org/10.4194/1303-2712-v16_3_01.
[73] Gundermann, K., Büchel, C., 2014. Structure and functional heterogeneity of fucoxanthin-chlorophyll proteins in diatoms. In: Hohmann-Marriott, M.F. (Ed.), The structural basis of biological energy generation. Springer Netherlands, Dordrecht, pp. 21–37. https://doi.org/10.1007/978-94-017-8742-0_2.
[74] Büchel, C., 2014. Fucoxanthin-chlorophyll-proteins and non-photochemical fluorescence quenching of diatoms. In: Demmig-Adams, B., Garab, G., Adams Iii, Govindjee, W. (Eds.), Non-photochemical quenching and energy dissipation in plants, algae and cyanobacteria. Springer Netherlands, Dordrecht, pp. 259–275. https://doi.org/10.1007/978-94-017-9032-1_11.
[75] Veith, T., Brauns, J., Weisheit, W., Mittag, M., Büchel, C., 2009. Identification of a specific fucoxanthin-chlorophyll protein in the light harvesting complex of photosystem I in the diatom Cyclotella meneghiniana. Biochim Et Biophys Acta (BBA) - Bioenerg 1787, 905–912. https://doi.org/10.1016/j.bbabio.2009.04.006.
[76] Ikeda, Y., Komura, M., Watanabe, M., Minami, C., Koike, H., Itoh, S., et al., 2008. Photosystem I complexes associated with fucoxanthin-chlorophyll-binding proteins from a marine centric diatom, Chaetoceros gracilis. Biochim Et Biophys Acta (BBA) - Bioenerg 1777, 351–361. https://doi.org/10.1016/j.bbabio.2008.01.011.
[77] Ikeda, Y., Yamagishi, A., Komura, M., Suzuki, T., Dohmae, N., Shibata, Y., et al., 2013. Two types of fucoxanthin-chlorophyll-binding proteins I tightly bound to the photosystem I core complex in marine centric diatoms. Biochim Et Biophys Acta (BBA) - Bioenerg 1827, 529–539. https://doi.org/10.1016/j.bbabio.2013.02.003.